










ORIGINAL ARTICLE

GATA1 pathogenic variants disrupt MYH10 silencing during megakaryopoiesis

Paul Saultier^{1,2}  | Sandrine Cabantous¹ | Michel Puceat³  | Franck Peiretti¹  |
 Timothée Bigot¹ | Noémie Saut^{1,4} | Jean-Claude Bordet⁵ | Matthias Canault¹  |
 Johannes van Agthoven⁶ | Marie Loosveld^{4,7} | Dominique Payet-Bornet⁷  |
 Delphine Potier⁷  | Céline Falaise^{2,4} | Denis Bernot¹ | Pierre-Emmanuel Morange^{1,4}  |
 Marie-Christine Alessi^{1,4}  | Marjorie Poggi¹ 

¹Aix Marseille Univ, INSERM, INRAe, C2VN, Marseille, France

²Department of Pediatric Hematology, Immunology and Oncology, APHM, La Timone Children's Hospital, Marseille, France

³Aix Marseille Univ, INSERM, MMG, Marseille, France

⁴APHM, CHU Timone, French Reference Center on Inherited Platelet Disorders, Marseille, France

⁵Unité d'Hémostase Biologique, Bron, France

⁶Structural Biology Program, Division of Nephrology/Department of Medicine, Massachusetts General Hospital and Harvard Medical School, Charlestown, MA, USA

⁷Aix-Marseille Univ, CNRS, INSERM, CIML, Marseille, France

Correspondence

Marie-Christine Alessi, C2VN, Faculté de Médecine Timone, 27 Boulevard Jean Moulin, 13385 Marseille, France.
 Email: marie-christine.alessi@univ-amu.fr

Funding information

Fondation pour la Recherche Médicale, Grant/Award Number: FDM20150633607; French Foundation for Rare Diseases, Grant/Award Number: WES 2012-2001; The National Institutes of Diabetes, Digestive and Kidney Diseases (NIDDK) of the National Institutes of Health, Grant/Award Number: DK101628

Abstract

Background: GATA1 is an essential transcription factor for both polyploidization and megakaryocyte (MK) differentiation. The polyploidization defect observed in GATA1 variant carriers is not well understood.

Objective: To extensively phenotype two pedigrees displaying different variants in the GATA1 gene and determine if GATA1 controls MYH10 expression levels, a key modulator of MK polyploidization.

Method: A total of 146 unrelated *propositi* with constitutional thrombocytopenia were screened on a multigene panel. We described the genotype-phenotype correlation in GATA1 variant carriers and investigated the effect of these novel variants on MYH10 transcription using luciferase constructs.

Results: The clinical profile associated with the p.L268M variant localized in the C terminal zinc finger was unusual in that the patient displayed bleeding and severe platelet aggregation defects without early-onset thrombocytopenia. p.N206I localized in the N terminal zinc finger was associated, on the other hand, with severe thrombocytopenia (15G/L) in early life. High MYH10 levels were evidenced in platelets of GATA1 variant carriers. Analysis of MKs anti-GATA1 chromatin immunoprecipitation-sequencing data revealed two GATA1 binding sites, located in the 3' untranslated region and in intron 8 of the MYH10 gene. Luciferase reporter assays showed their respective role in the regulation of MYH10 gene expression. Both GATA1 variants significantly alter intron 8 driven MYH10 transcription.

Conclusion: The discovery of an association between MYH10 and GATA1 is a novel one. Overall, this study suggests that impaired MYH10 silencing via an intronic regulatory element is the most likely cause of GATA1-related polyploidization defect.

Manuscript handled by: Matthew T. Rondina

Final decision: Matthew T. Rondina, 24 May 2021

© 2021 International Society on Thrombosis and Haemostasis

KEYWORDS

downstream targets, functional variants, GATA1, MYH10, platelets

1 | INTRODUCTION

GATA1 is an essential transcription factor for erythrocyte and megakaryocyte (MK) differentiation.^{1,2} It belongs to the GATA family of zinc finger (ZF) transcription factors, which recognize the W(A/T)GATAR(A/G) DNA pattern. The protein is encoded by the *GATA1* gene, located on the X chromosome.^{3,4} The GATA1 protein contains two highly conserved ZFs, which are separated by a short linker. The C-terminal ZF binds with high affinity and specificity to (A/T)GATA(A/G) motifs throughout the genome, whereas the N-terminal ZF can bind protein cofactors, such as FOG1.

Several hemizygous loss-of-function *GATA1* variants have been described in patients with varying degrees of macrothrombocytopenia and anemia. Most of these variants affect the N-terminal ZF of GATA1 and impair the GATA1 DNA binding interaction with the GATA1 cofactor FOG1.⁵⁻⁷ Accordingly, mice with targeted mutations in the *Gata1* promoter display macrothrombocytopenia, in which reduced *Gata1* expression⁸⁻¹⁰ or conditional knockout of *Gata1* results in a selective loss of *Gata1* expression in MKs.¹¹ This observation underscores the importance of GATA1 in sustaining normal megakaryocytic differentiation and platelet production. Previous studies have shown that *GATA1* is required for both polyploidization and MK differentiation. Bone marrow from *GATA1* variant carriers shows a moderate to marked increase in MK numbers, which are also small and hypobulbated.^{5,6} *In vivo*, the *Gata1*^{low} mice display a marked increase in small and hypoploid MKs.⁹ *GATA1*-deficient MKs also exhibit increased proliferation both *in vitro* and *in vivo* with defective nuclear and cytoplasmic maturation.^{9,10}

Some studies have suggested that the polyploidization defect is associated with *GATA1* inactivation through deregulation of cyclin D1, STAT1, or CDC6 expression.^{10,12} However, we propose an alternative mechanism involving altered silencing of the protein non-muscle heavy chain IIB (MYH10). During polyploidization, expression of MYH10 protein, which localizes to the actomyosin contractile ring, is repressed by the transcription repressor RUNX1, thereby enabling the switch from mitosis to endomitosis.¹³ The polyploidization defect observed in *RUNX1* variant carriers is in part associated with the persistence of MYH10 expression,¹⁴ which has been detected in circulating platelets.¹⁵ Similarly, increased levels of MYH10 protein have been detected in platelets from patients carrying *FLI1* variants, thus suggesting cooperation between the two transcription factors, RUNX1 and FLI1, in normal repression of the *MYH10* gene.¹⁵⁻¹⁸

Genome-wide analysis of simultaneous *GATA1*, *RUNX1*, *FLI1*, and *TAL1* DNA binding in human MKs has revealed that these transcription factors bind to the same binding sites in the genome and cooperate to regulate the expression of target genes during the early stages of megakaryopoiesis.¹⁹ Transcriptional cooperation between *RUNX1* and *GATA1* in the activation of megakaryocytic

Essentials

- MYH10 silencing is an essential step in the megakaryocyte polyploidization.
- Two novel *GATA1* variants were identified in the N and C-terminal zinc finger domain.
- MYH10 expression levels are increased in platelets from both *GATA1* variant carriers.
- *GATA1* alters MYH10 expression via an intronic binding site in the *MYH10* gene.

promoters has been further established using reporter assays with transient transfection in a variety of mammalian cell lines. These studies have demonstrated the physical interaction between the two transcription factors.^{20,21} Therefore, we suggest that deregulation of *MYH10* expression may also be implicated in *GATA1*-related thrombocytopenia.

In this study, we report a detailed analysis of two novel *GATA1* variants localized in each ZF. Elevated MYH10 protein levels were found in platelets from carriers of each variant. We describe the identification of a *MYH10* intronic region that functions as a *GATA1*-responsive cis-regulatory element.

2 | MATERIALS AND METHODS

Methods concerning high-throughput gene sequencing, structural model of *GATA1*-DNA interactions, flow cytometry analysis, cell expression, and luciferase reporter assays, platelet-rich plasma (PRP) serotonin level, platelet PAI-1 level, mepacrine uptake and release, immunoprecipitation and western blot analysis, and epifluorescence microscopy are described in the Online Supplementary Material.

2.1 | Study limitations

Owing to the limited number of patients, statistical comparison between patients and controls was not always possible. Fresh whole blood (required for primary cell culture) was available in only one patient (F1-II1). Consequently, most *in vitro* experiments were performed using transfected nonhematopoietic cell line. The platelet serotonin levels were available for two patients and the bone marrow smears for one patient. Transmission electron microscopy (TEM) analysis of platelets was performed for only one family. The other experiments were performed for all patients.

2.2 | Patient enrollment, research ethics, patient consent, and clinical and laboratory data

From 2014 to 2017, we recruited 146 unrelated *propositi* with constitutional thrombocytopenia of unknown origin. Genetic analyses were performed at the French Reference Center for Inherited Platelet Disorders at La Timone University Hospital in Marseille, France. All cases were included in the study after obtaining informed written consent in accordance with protocols approved by national institutional review boards and Declaration of Helsinki principles. Medical and family history data were obtained from medical reports and patient interviews. Bleeding tendency was assessed using the International Society on Hemostasis and Thrombosis-Bleeding Assessment Tool score. Red blood cell counts, platelet counts, mean corpuscular volume (MCV), and mean platelet volume were determined on EDTA-anticoagulated blood samples using the ADVIA 120 automated cell counter. Bone marrow smears were obtained for one *propositus* and stained with May-Grünwald-Giemsa. Fetal hemoglobin levels were assessed using high-performance liquid chromatography in the Biochemistry Department at La Timone University Hospital in Marseille, France.

2.3 | Platelet aggregation

Platelet aggregation was assessed by measuring light transmission through the stirred PRP suspensions for 3 min using an APACKT 4004 aggregometer. Platelet aggregation was triggered by adding 1 μ M or 2.5 μ M adenosine diphosphate (ADP; Helena Laboratories), 0.5 mg/ml arachidonic acid (Helena Laboratories) and 0.36 μ g/ml or 0.72 μ g/ml collagen (Bio/Data Corporation). Platelet agglutination was triggered by adding 1.5 mg/ml ristocetin (Sigma-Aldrich).

2.4 | Evaluation of platelet granules using electron microscopy

TEM analysis of platelets was performed as previously described.¹⁸ Briefly, we assessed platelet surface area (μm^2) and diameter (μm), the number of alpha granules per unit area (μm^{-2}), and the diameter of alpha granules in a blinded case/control experiment. Dense granules were quantified using whole-mount electron microscopy as previously described.¹⁸

2.5 | *In vitro* megakaryocyte differentiation and ploidy

After density gradient separation (Eurobio), circulating CD34⁺ cells were purified using positive selection with magnetic beads (Miltenyi-Biotec) and cultured in StemSpan Serum-Free Expansion Medium II supplemented with Megakaryocyte Expansion Supplement (Stemcell Technologies). At days 9 and 11 of culture, MKs were analyzed via

flow cytometry for CD41 and CD42a markers (anti-CD41-APC and anti-CD42a-PE antibodies; BD Biosciences) as well as for DNA ploidy using Hoechst-33342 (Sigma-Aldrich). The cells were then analyzed using a Navios cytometer (Beckman Coulter).

2.6 | Statistical analyses

Quantitative variables are expressed as the mean \pm standard error. Analyses were performed using GraphPad Prism software. Statistical differences were determined via analysis of variance (ANOVA) with Dunnett's multiple comparison test. $p < 0.05$ was considered statistically significant.

3 | RESULTS

3.1 | Two novel GATA1 variants identified via genetic analysis

Next-generation sequencing yielded the identification of two novel GATA1 variants (NM_002049) in three boys from two unrelated families (Figure 1A,B). For the first family, only one hemizygous variant c.617A>T (p.N206I) causing alteration in the N-terminal ZF was evidenced in the proband (II-1) (Figure 1A). For the second family, only one deleterious variant c.802C>A (p. L268M) was shared by the two brothers in the C terminal ZF GATA1 domain. Five other variants worn by the two brothers have been identified. None of them were pathogenic because of benign *in silico* prediction and/or high allelic frequency ($>10^{-4}$) in general population databases (Table S1). The analysis of the coverage of these genes was also not in favor of deletion or duplication (data not shown). These two missense variants were absent from the GnomAD and ExAC databases, and have a Combined Annotation Dependent Depletion (CADD) score of 24.9 for c.617A>T (Request: Chromosome X, Position 48792341, CADD GRCh38-v1.6) and 23.7 for c.802C>A (Request: Chromosome X, Position 48793229, CADD GRCh38-v1.6). The chart prediction for these two variants based on different prediction tools to identify disease relevant nonsynonymous single nucleotide variants is given in supplementary figures (Figure S1A and B). The variants occurred in both mothers, although as expected, the two fathers were homozygous for wild-type genotypes (Figure 1A).

3.2 | Structural modeling

Structural analysis provided further insight into the mechanisms by which these two variants may exert deleterious effects. An initial sequence alignment of GATA1 orthologs and paralogs revealed that both variants affect highly conserved sequences and may therefore play a structural role in GATA1 binding to target DNA sequences or protein-binding partners (Figure S1). As shown in the X-ray structure of GATA1 in complex with double-stranded DNA, the L268 residue

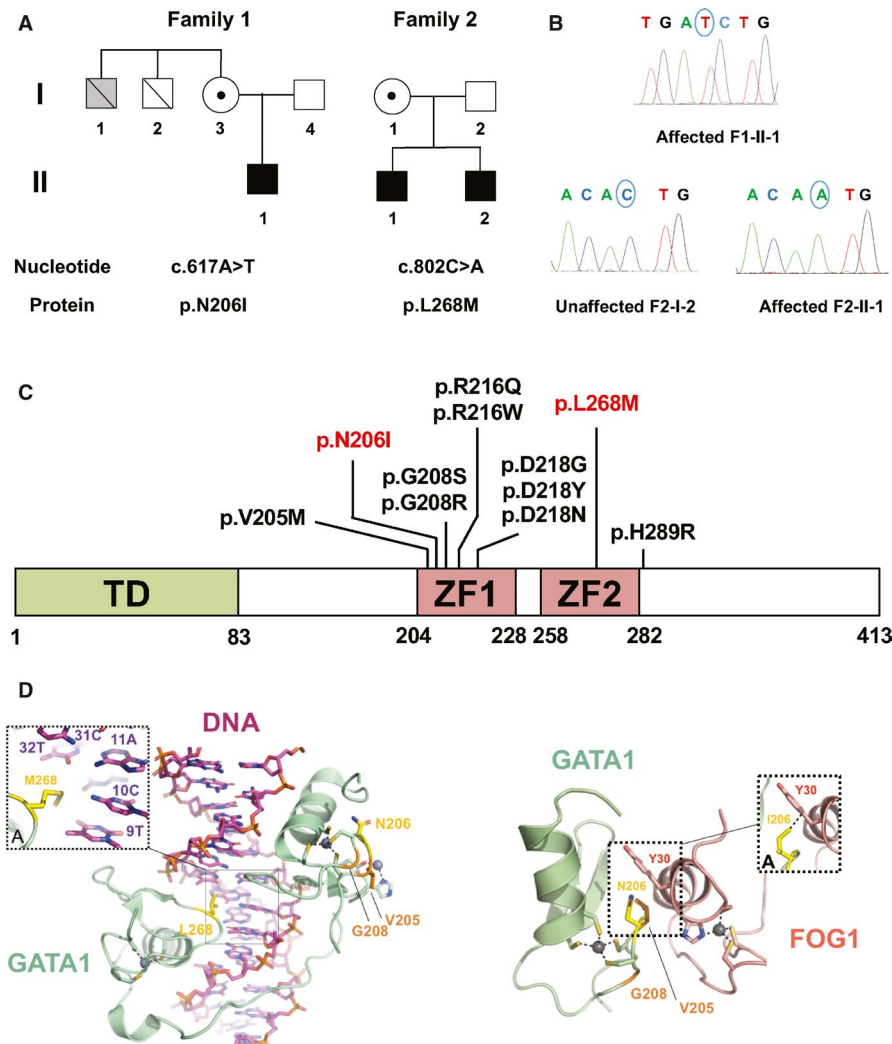


FIGURE 1 Identification of two novel GATA1 variants. **A**, Pedigrees of the affected families. Squares denote males; circles represent females; slashes denote deceased family members; solid black symbols represent affected family members carrying a hemizygous GATA1 variant; circles with a dot represent heterozygous female carriers of the variants; solid gray symbols represent nontested family members with a medical history of bleeding events. **B**, Sanger sequencing electropherograms of the indicated family members. **C**, Schematic diagram of the GATA1 protein domain structure. The functional N-terminal transactivation domain (TD) and both the N- and C-terminal zinc-finger domains (ZF1 and ZF2, respectively) are depicted. The positions of the variations within GATA1 are indicated in red (variations reported in this study) and black (variations reported in previous studies). **D**, Left: structure of Zn fingers of GATA1 bound to palindromic DNA recognition site (PDB code: 3VD6). The diagram shows GATA1 in green cartoon with key residues L268 and N206 in yellow sticks, and the DNA fragment in magenta sticks. Zn²⁺ ions are in gray spheres with stick representation of coordinating residues. Other GATA1 relevant variants V205M and G208R are mapped in orange sticks. Inset A shows 3VD6 superimposed to the same structure harboring a model of the L268M mutation. Right: Lowest energy conformer of NMR structure of Zn fingers of GATA1 bound to FOG1 (PDB code: 1Y0J). The diagram shows GATA1 in green cartoon with key residue N206 in yellow stick, and FOG1 in red. Zn²⁺ ions are in gray spheres with stick representation of coordinating residues. Other GATA1 relevant variants V205M and G208R are mapped in orange sticks. Inset A shows 1Y0J superimposed to the same structure harboring a model of the N206I mutation. In dashes is shown an atomic clash between I206 (GATA1) and Y30 (FOG1) with interatomic distances below 2.5 Å

is located in the interface between GATA1 and the major groove of the DNA-binding sequence TGATAA (Figure 1D, left), making van der Waals contact with bases 32T, 33T, 9T, and 10C (distance cut-off of 4 Å). Structural modeling of the p.L268M substitution did not reveal any steric hindrance at the GATA1-DNA interface. However, the loss-of-function effect of p.L268M likely results from distorted hydrophobic packing with the aforementioned bases (shown in the left inset of Figure 1D).

Although the N206 residue is not localized within the GATA1-DNA interface (Figure 1D, left), the p.N206I substitution may affect the capacity of GATA1 to bind to FOG1. The nuclear magnetic resonance structures of the GATA1-FOG1 complex revealed that the N206 residue is part of the interface between the two proteins, forming a specific amino- π interaction between the GATA1 side chain amino group and the aromatic ring of FOG1-Y30 (Figure 1D, right). Structural modeling showed that this interaction

is disrupted in the N2016I variant. The variant caused destabilization of the GATA1/FOG1 interface by steric hindrance, likely resulting in FOG1-mediated loss of function (shown in the right inset of Figure 1D).

3.3 | Nuclear localization and FOG1 binding in GATA1 cases

To further investigate the subcellular localization of the GATA1 variants, we expressed the wild-type and variant forms of GATA1 in MSR and H9C2 cells. GATA1 variants did not reduce GATA1 protein levels (data not shown). The GATA1 variants entered the nucleus to the same extent as wild-type GATA1 (Figure S2A), suggesting that the variants alter GATA1 binding properties to chromatin rather than subcellular localization. The structural prediction was confirmed via GATA1 coimmunoprecipitation using MSR cells overexpressing GATA1 (wild-type or variants) and FOG1. FOG1 was detected in the GATA1 precipitates of wild-type and p.L268M GATA1-expressing cells, whereas FOG1 detection was markedly reduced in the p.N206I GATA1 precipitates (Figure S2B).

3.4 | Case descriptions

Thrombocytopenia onset kinetics markedly differed between the two families. Thrombocytopenia was present early in life in the p.N206I carrier (F1-II-1) with a severely reduced platelet count (15 G/L) at the age of 18 months that persisted. Bleeding during dental avulsion was prevented by platelet concentrate transfusion before the procedure. The patient was referred to our reference center on platelet disorders because of resistance to immunoglobulin, corticosteroids, and mycophenolate mofetil treatment because immune thrombocytopenia was initially suspected. The F1 proband did not suffer from anemia (hemoglobin 118 g/L at 7 years of age), and his mean corpuscular volume was rather low (76.8 fL; normal range: 80-95 fL). May-Grunwald-Giemsa staining of bone marrow smears showed mild dyserythropoiesis with erythroblastosis and nuclear karyorrhexis (Figure 2C).

By contrast, thrombocytopenia was initially absent in the two F2 brothers carrying the p.L268M variant. At 18 and 9 months of age, F2-II-1 and F2-II-2 exhibited normal platelet counts (261 G/L and 233 G/L), respectively, despite pronounced mucocutaneous bleedings. The initial hemostasis assessment in the two children showed no defects in coagulation (normal prothrombin and activated partial thromboplastin times, normal levels of the factors VIII, XIII, fibrinogen, and von Willebrand factor) or fibrinolysis (normal alpha2 antiplasmin, t-PA, and plasma PAI-1 levels, and normal von Kaulla test) (data not shown). Bleeding time was prolonged (>15 min) and was not corrected by DDAVP injection. A severe platelet aggregation defect was detected in both brothers with normal platelet counts in PRP samples (338-380G/L). On

several occasions (six times for the older brother and three times for the younger brother) and in the absence of medication, collagen, arachidonic acid, and TXA2 agonist U-46619 failed to induce platelet aggregation. Reduced platelet aggregation was also observed in response to ADP, whereas ristocetin-induced agglutination was almost normal (Table 1 and Figure S3). Both boys were diagnosed with hereditary platelet dysfunction. Diagnosis of Glanzmann thrombasthenia has been evoked but platelet exploration has refuted it. Indeed, platelet aggregation was only slightly reduced upon stimulation with high-dose ADP (10 μ M) and TRAP-14 (50 μ M). Exploration of GPIIb/IIIa with flow cytometry showed a normal expression level of GPIIb/IIIa (Table 2) and a significant increment of PAC-1 fixation after 10 μ M ADP stimulation (mean fluorescence intensity: basal state = 0.31 [normal value 0.21-0.49] stimulated state = 6.23 [normal value: 5.4-16.2], positive cell: basal state = 0% [normal value <5%], stimulated state = 73% [normal value >70%]). In addition, we did not detect variations, deletion, or duplication in the *ITGA2B* and *ITGB3* genes and in genes involved in its activation (*FERMT3*, *RASGRP2*, *TLN1*). The altered aggregation profiles were not the result of defective expression of GPVI, SYK, PLC γ 2, or COX1 in platelets, with no major differences in signal intensity between the two parents and the children. A 30% reduction in TBXAS1 levels was observed in both F2 children compared with their parents (Figure S4). In patient F2-II-2, dental avulsions and an appendectomy were performed after platelet concentrate transfusions without hemorrhagic complications. At 5 years of age, the platelet counts for patient F2-II-1 remained in the normal range ($194 \times 10^9/L$), whereas his brother's platelet counts started to decrease at 3 years of age ($131 \times 10^9/L$). Thrombocytopenia then gradually developed over time in both brothers, with more severe thrombocytopenia in the younger boy (F2-II-2) (Figure 2A). TEM analysis of platelets derived from patient F2-II-1 showed that, in keeping with previous measurements of mean platelet volume obtained using hematology analyzers, the platelet size distribution was normal (Figure 3B and Table S1).

Because GATA1 is critical for erythropoiesis, we also aimed to identify any red blood cell defects. Examination of peripheral F2-II-2 blood smears demonstrated abnormally shaped red blood cells with anisocytosis and poikilocytosis (Figure 2B). The F2 probands did not suffer from anemia either, with hemoglobin levels at 111 and 112 g/L at 5 years of age and 146 and 144 g/L at the date of last follow-up (at 27 and 23 years of age, respectively). Hemoglobin electrophoresis revealed, as already reported in several GATA1-related diseases, an elevated level of fetal hemoglobin. They both presented with elevated fetal hemoglobin levels (25%), albeit without microcytosis (MCV: 87-92 fL between 5 and 8 years of age) and hypochromia (mean corpuscular hemoglobin concentration: 330-331 g/L between 5 and 8 years of age). Remarkably, the two F2 brothers displayed a progressive increase in MCV over time, whereas their platelet counts gradually decreased (Figure 2A); the values at last follow-up were 99 and 103 fL (at 26 and 23 years of age, respectively). Table 3 resumes main characteristics of GATA1 variant carriers.

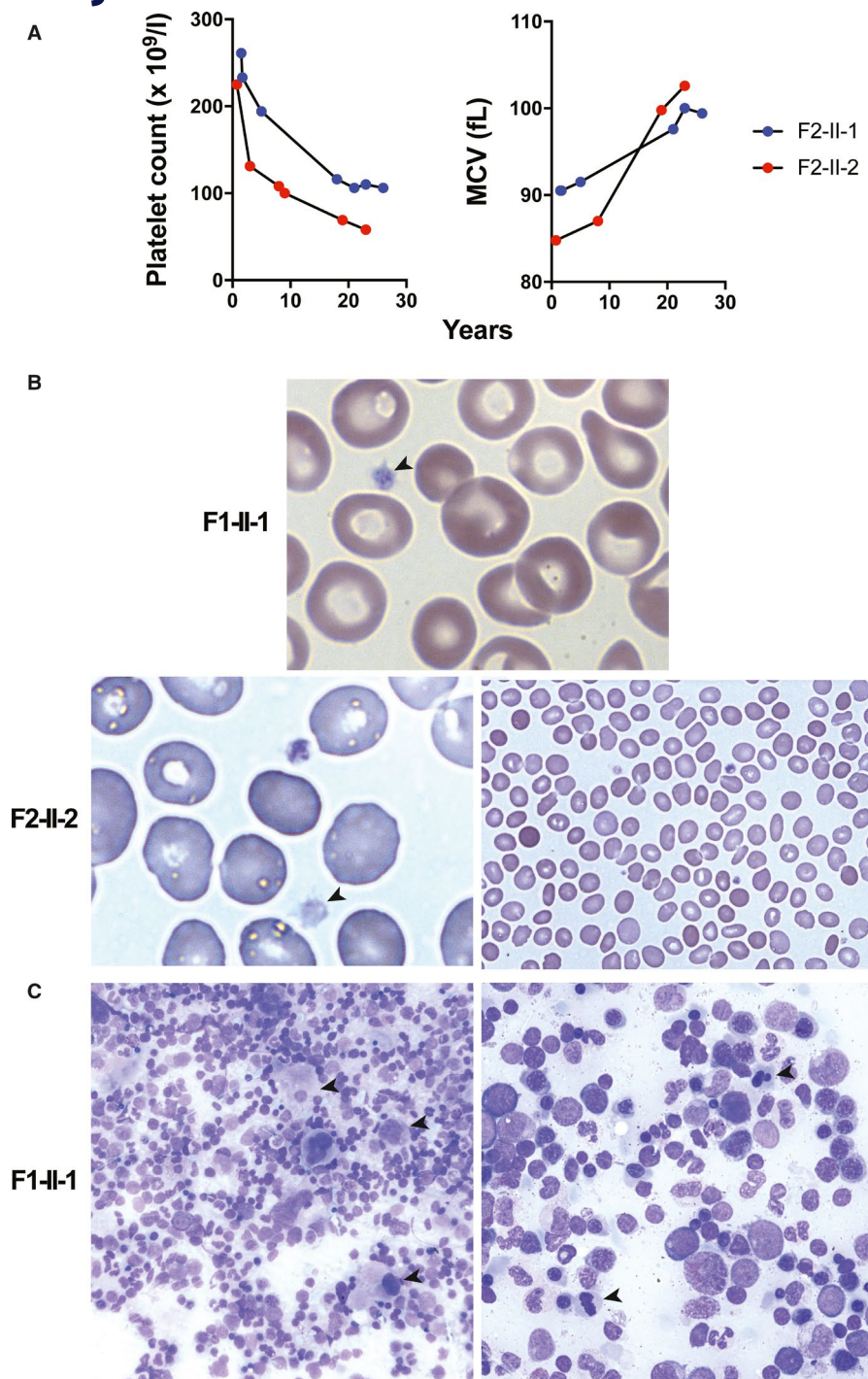


FIGURE 2 Quantitative and morphological modifications of platelets and red blood cells in GATA1 variant carriers. **A**, Evolution of platelet count and mean corpuscular volume (MCV) of erythrocytes with age in the two F2 probands. **B**, Representative images of peripheral blood smears stained with May-Grünwald-Giemsa for patients F1-II-1 and F2-II-2 (at 6 and 23 years old, respectively). The peripheral blood smear images revealed hypogranular platelets (left, black arrow, magnification $\times 1000$) mild anisocytosis and poikilocytosis (right, magnification $\times 500$). **C**, Representative images of bone marrow aspirate smears stained with May-Grünwald-Giemsa for patient F1-II-1 (at 17 months old). Assessment of bone marrow aspirates revealed dysmegakaryopoiesis with hypolobulated megakaryocytes (left, black arrow, magnification $\times 200$) and dyserythropoiesis with nuclear karyorrhexis (right, black arrow, magnification $\times 500$). Smears were examined for each subject by a well-trained hematologist (M. Loosveld)

3.5 | Platelets from GATA1 cases present severe dense granular defect

Electron microscopy revealed a major delta granular deficit in GATA1 variant carriers. Analysis via whole-mount electron microscopy revealed reduced numbers of dense granules, with an average of 0.44 ± 1.02 (F1-II-1), 0.56 ± 0.97 (F2-II-1), and 0.13 ± 0.49 (F2-II-2) dense granules per platelet (normal values: 5.46 ± 3.91). Furthermore, 77% (F1-II-1), 65% (F2-II-1), and 90% (F2-II-2) of platelets lacked dense granules (Figure 3A). Mepacrine uptake and release upon TRAP-14 stimulation ($40 \mu\text{M}$) and quantification of mepacrine-labeled dense granules via

fluorescent microscopy confirmed the dense granule defect in all variant carriers (Figure S5). On several occasions, we observed low platelet serotonin levels for the two F2 brothers (F2-II-1: $0.12 \mu\text{g}/109$ platelets in 2015, $0.10 \mu\text{g}/109$ platelets in 2009, and F2-II-2: $0.16 \mu\text{g}/109$ platelets in 2015; normal range: $0.3\text{--}1.2 \mu\text{g}/109$ platelets). Flow cytometry showed reduced expression levels of the dense granule marker CD63 upon TRAP-14 stimulation in all variant carriers (Table 2).

Platelet count (Table 1), platelet aggregation (Figure S3), flow cytometric evaluation of mepacrine uptake and release (not shown) and platelet serotonin levels ($0.39 \mu\text{g}/109$ platelets; normal range: $0.3\text{--}1.20 \mu\text{g}/109$ platelets) were normal in the mother (F2-I-1).

TABLE 1 Platelet aggregation assays

Individuals	Age (y)	Blood Platelet Count ($\times 10^9/L$)	PRP Platelet Count ($\times 10^9/L$)	Platelet Aggregation Maximal Intensity (%)					
				ADP		Collagen		Arachidonic Acid	Ristocetin
				1 μ M	2.5 μ M	0.36 μ g/ml	0.72 μ g/ml	0.5 mg/ml	1.5 mg/ml
Control*	NA	NA	350	45	68	60	63	69	76
F2-II-1	1.7	233	380	9	25	0	0	19	67
Control*	NA	NA	350	45	68	57	63	69	68
F2-II-2	0.8	225	338	8	23	0	0	11	46

Individuals	Age (y)	Blood Platelet Count ($\times 10^9/L$)	PRP Platelet Count ($\times 10^9/L$)	Platelet Aggregation Maximal Intensity (%)					
				ADP		Collagen		Arachidonic Acid	Ristocetin
				2.5 μ M	5 μ M	10 μ M	3.3 μ g/ml	0.5 mg/ml	1.25 mg/ml
Normal range				83-93	75-90	78-92	79-85	76-91	78-948
F2II-1	26.7	106	159	40	62	56	25	14	73
F2II-2	22.7	58	102	40	62	68	24	11	70

Results correspond to assays performed in 1990 and 1993 (A) and 2015 (B).

NA, not available; PRP, platelet-rich plasma.

*Controls correspond to one healthy individual tested at the same time.

TABLE 2 Platelet glycoprotein expression

Platelet Glycoprotein MFI (a.u.)	Individuals				Normal Range (10th-90th range n = 12)
	F1-II-1	Normal Range (10th-90th range n = 14)	F2-II-1	F2-II-2	
α IIb β 3 (CD41)					
Basal	24	21-44	24	30	20-29
TRAP14 50 μ M	25	30-62	30	34	28-46
GPIIb α (CD42b)					
Basal	1.7	1.2-.3	2.1	2.4	1.2-2.4
TRAP14 50 μ M	1.5	0.9-2.3	1.8	1.8	0.6-1.1
CD63					
Basal	1.2	0.9-3.4	1.1	1.3	0.5-1
TRAP14 50 μ M	1.6	1.9-6.3	1.7	1.3	1.3-3.6
Ratio TRAP-14 / basal	1.3	1.7-3.7	1.4	1	1.5-4.8
CD62P (P-selectin)					
Basal	0.2	0.09-0.35	0.2	0.4	0.15-0.75
TRAP14 50 μ M	0.2	1.9-6.3	1.5	1.7	2.3-5
Ratio TRAP-14 / basal	1.1	12.4-22.8	7	4.2	5.5-25

3.6 | Platelets from GATA1 cases present mild alpha granular defect and structural abnormalities

Assessment of peripheral blood smears from F1-II-1 and F2-II-2 did not show gray platelets, although an experienced hematologist identified some hypogranular platelets in both children (Figure 2B).

Quantitative morphometric evaluation of F2-II-1 alpha granules indicated a distinct decrease in alpha granule density and consequently a decrease in the alpha granule area: total platelet area ratio (4.1%; reference range 11.0%-13.5%). The diameter of the alpha granules was only slightly decreased. The platelets presented many other structural anomalies. Platelet sections showed highly variable granular and mitochondrial content, with large areas of

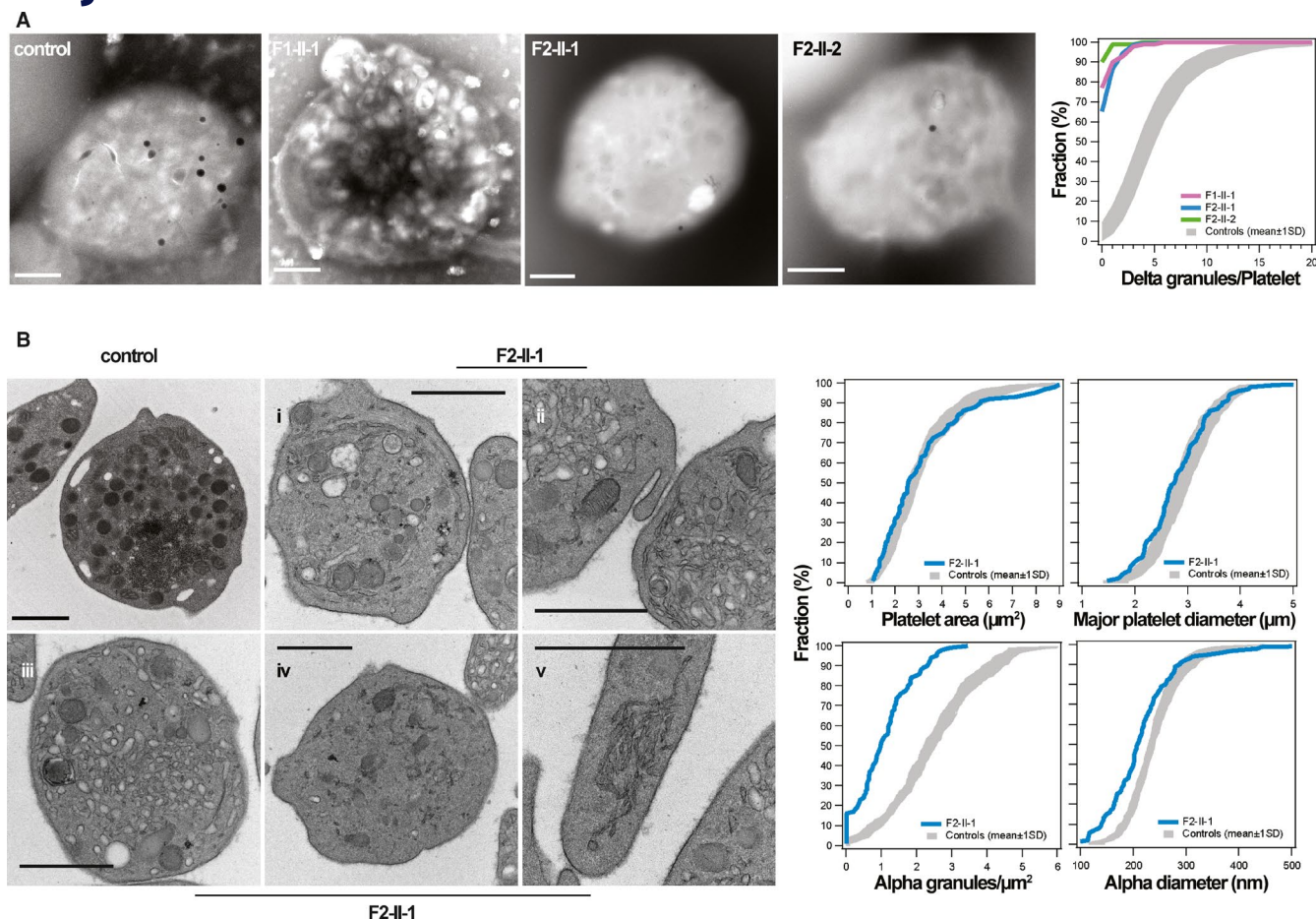


FIGURE 3 Alpha and dense granule defects associated with GATA1 variants. **A**, Representative micrographs of dense granule distribution in a control and patients F1-II-1 (at 8 years old), F2-II-1 (at 27 years old) and F2-II-2 (at 23 years old). Scale bar: 1 μm . The graph shows the cumulative distribution of dense granules per whole platelet deposited on formvar film for patient vs. control platelets (healthy subjects, $n = 54$); 100 platelets per whole-platelet mount were examined for each subject by a well-trained engineer blinded to the genotype (J.C. Bordet, Unité d'Hémostase Biologique, Bron, France). **B**, Platelet sections from a healthy subject (control panel) and patient F2-II-1 (all other panels). Platelet section from control shows numerous alpha granules, mitochondria recognizable by the crests, and a large glycogen area. Although the numbers are variable, platelets derived from patient F2-II-1 at 22 years old displayed low alpha granule counts for each section, sometimes lower than mitochondria counts. Overall, the sections display either very few organelles with a relatively amorphous background (i) or normal counts for organelles that show variable granulation (iv). Other notable structures observed included very large areas of membrane complexes (ii, iii) and apoptotic granules (left part of panel iii). We also observed membranous formations that resemble a dense tubular system, although the formations were occasionally arranged in a large ring (ii), in the vicinity of the tubulin circle (bottom center panel) or in aggregates in the cytoplasm (v). Scale bar: 0.5 μm . The graphs show the cumulative distribution of platelet area, number of alpha granules/ μm^2 , major platelet diameter, and alpha granule diameter using classical electron microscopy sections in patient F2-II-1 vs. control platelets (healthy subjects $n = 10$); we examined 100 platelets per section

membrane complexes that in some cases occupied the entire section (see Figure 3B legend for complete description). To further assess the alpha granules, we evaluated the levels of PAI-1 antigen in serum. Indeed, 95% of circulating PAI-1 is localized in platelets.²² Furthermore, proteomic analysis has found that reduced PAI-1 levels is a feature of gray platelet syndrome.²³ For the three patients, PAI-1 levels were in the normal range (F1-II-1: 0.35; F2-II-1: 0.76; and F2-II-2: 0.69; normal range 0.33-1.07 ng/106 platelets). Flow cytometry showed moderate decrease in the levels of the alpha granule protein marker CD62P upon TRAP-14 stimulation in both the F2 children, whereas CD62P did not change after TRAP-14 stimulation in the F1-II-1 (Table 2).

3.7 | GATA1 variants are associated with abnormal megakaryocyte maturation and polyploidization

Microscopic evaluation of bone marrow aspirate smears from patient F1-II-1 showed normal numbers of MKs with a high proportion of round or hypolobulated polyploid nuclei (Figure 2C) indicating abnormal maturation. We further analyzed MK development using blood-derived CD34⁺ stem cells. The F1 carriers exhibited a 12- to 48-fold increase in circulating CD34⁺CD38⁺CD45^{low}CD19^{low} cells ($n = 2$) compared with healthy controls ($n = 5$) (Figure 4A). Analysis of CD41⁺ and CD42a⁺ cells at days 9 and 11 revealed a marked reduction in MK differentiation with reduced cell size compared with two

TABLE 3 Characteristics of GATA1 variant carriers

	Family 1 (F1-II-1)	Family 2 (F2-II-1 and F2-II-2)
DNA change	c.802C>A	C617A>T
Protein change	p.N206I	p.L268M
Variant localization	N-terminal zinc finger	C-terminal zinc finger
Clinical manifestations		
Thrombocytopenia	Early in life (18 months) with a severely reduced platelet count (15 G/L)	Initially absent (at 18 and 9 months, 261 and 233 G/L for each brother). Thrombocytopenia gradually developed from 2 to 5 years of age and then steadily worsened
Bleeding	Frequent bruising, post vaccinal hematoma	Pronounced mucocutaneous bleedings
	Bleeding during dental avulsion prevented by platelet concentrates	Bleeding during dental avulsion and appendicectomy was prevented by platelet concentrates
Platelet	Not done	Bleeding time >15 min
	No aggregation test performed (because platelet number is <20 G/L)	Aggregation defect (mainly collagen and arachidonic acid) in absence of thrombocytopenia
	> 90% reduction in dense granule number	≥ 90% reduction in dense granule number for both children
	Surface glycoproteins: No basal defect in CD41, CD42b, CD62P, and CD63; reduced expression levels of CD63 and CD62P after TRAP-14 stimulation	Surface glycoproteins: No basal defect in CD41, CD42b, CD62P, and CD63; reduced expression levels of CD63 and CD62P after TRAP-14 stimulation
	Serotonin: NA (too low platelet count)	Serotonin low values in both children: 0.12–0.16 µg/10 ⁹ platelets (Normal values: 0.3–1.20)
Coagulation and fibrinolysis	PAI-1 antigen: normal value, 0.35 ng/10 ⁶ platelets (Normal values: 0.33–1.07)	PAI-1 antigen: normal values in both child 0.69–0.76 ng/10 ⁶ platelets (Normal values: 0.33–1.07)
	No defect	No defect
Erythrocyte	Absence of anemia	Absence of anemia
	MCV: 77–81 fL (Normal values: 80–95)	Progressive increase in MCV over time (from 85–90 to 99 and 103 fL at 26 and 23 years of age) (Normal values: 80–95)
	Discrete anisopoikilocytosis, few dacryocytes and schizocytes	Anisopoikilocytosis
Bone marrow	Fetal hemoglobin not evaluated	Elevated level of fetal hemoglobin (25%)
	Dysmegakaryopoiesis with hypobulbated megakaryocytes and mild dyserythropoiesis with nuclear karyorrhexis	Not done

a.u., arbitrary unit; MFI, mean fluorescence intensity.

controls (Figure 4B,C). The CD41⁺CD42a⁺ population was almost absent in the F1-II-1 cells (Figure 4B). Furthermore, the percentage of high-ploidy cells (≥ 4n) in the F1-II-1 sample was reduced at day 9. The relative frequencies of 2n, 4n, 8n, and 16n ploidy MKs were 54% to 58%, 23% to 27%, 4% to 8%, and 1% to 2% in the controls, versus 66%, 18%, 0%, and 0% in the patient carrying the GATA1 variant, respectively (Figure 4D). Bone marrow smears and MK cultures were not available for the F2 family.

3.8 | GATA1 cases display increased MYH10 levels in platelets

To further investigate the effect of the GATA1 variants on MYH10, which is required for MK polyploidization and maturation, MYH10 levels were assessed in platelets derived from patients and healthy subjects. MYH10 protein was not detected in healthy donor platelets via immunoblotting. By contrast, MYH10 expression was detected

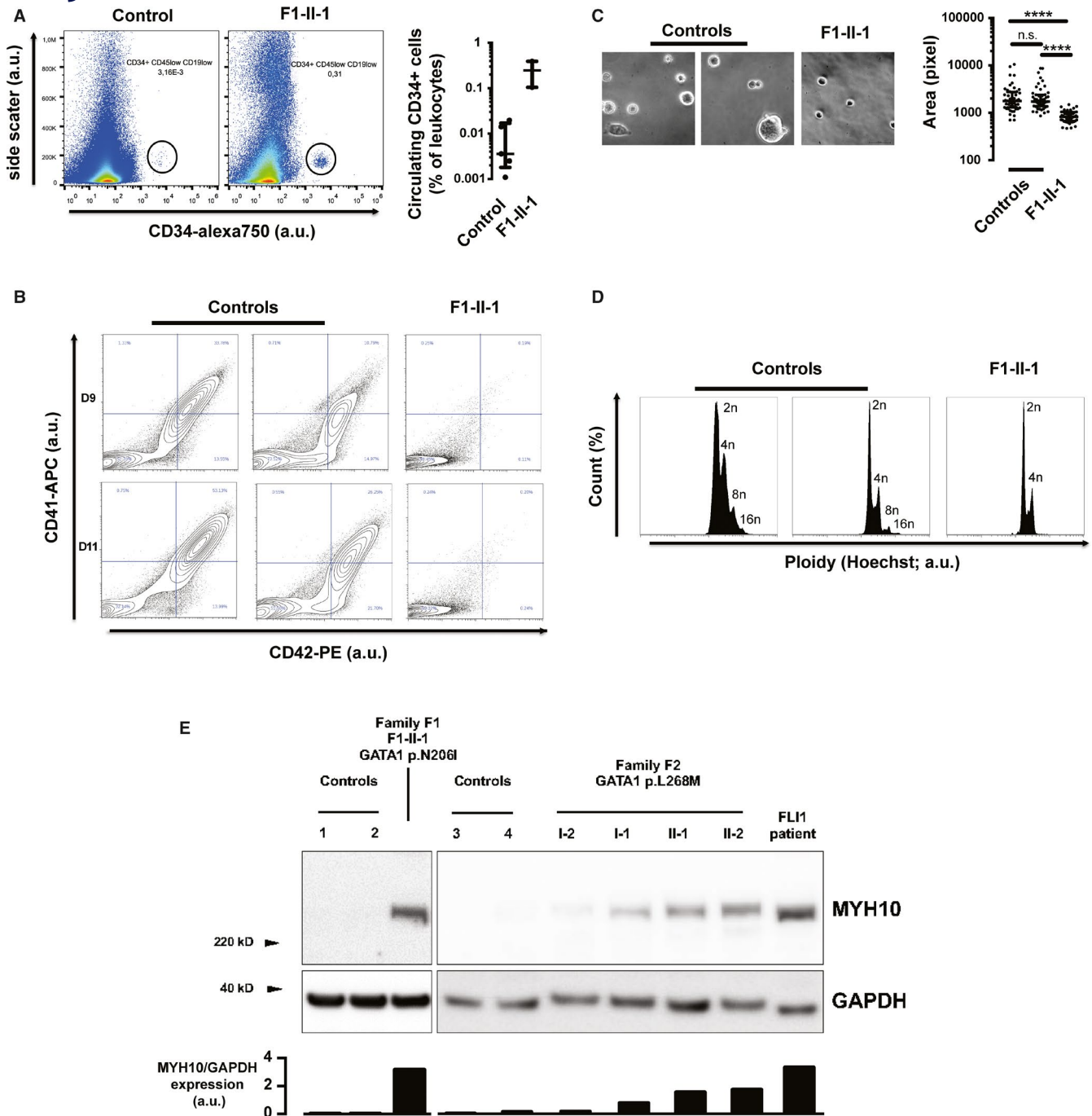


FIGURE 4 Increased number of CD34⁺ cells and abnormal megakaryocyte differentiation in GATA1 variant carriers. **A**, Flow cytometry analysis of circulating CD34⁺ cells. Left: Representative dot plots of cells from one healthy control and patient F1-II-1. The plots display the side scatter and CD34 expression analysis in CD19^{low} CD45^{low} cells. The ellipse gates show the CD19^{low} CD45^{low} CD34⁺ cell population. Right: The percentage of CD34⁺ cells in the total CD19^{low} CD45^{low} cell population. The control data represent five different individuals. The data for patient F1-II-1 were obtained from two independent experiments carried out at 15-month intervals. The data are provided as the median \pm interquartile range. **B-D**, In vitro megakaryocyte differentiation. Circulating CD34⁺ cells from F1-II-1 patient or controls were isolated and cultured in the presence of TPO and SCF to induce megakaryocytic commitment. **(B)** Megakaryocyte differentiation was monitored via flow cytometry. The density plots display the CD41/CD42a expression profiles of two unrelated controls and F1-II-1 affected patient (at days 9 and 11 of differentiation). **(C)** Representative images of cultured cells at day 11 ($\times 20$ magnification). The graph represents the median \pm interquartile range of the cell surface area. Fifty cells were quantified. Differences between the groups were assessed using the Kruskal-Wallis test followed by Dunn's multiple comparison test. **D**, Ploidy levels were monitored via flow cytometry. The histograms display the frequency distribution of Hoechst 33342 levels in CD34⁺-derived cells from two unrelated controls and F1-II-1 affected patient at day 9 of differentiation. **E**, Western blot analysis of MYH10 expression in platelets from the patients with GATA1 variants (F1-II2, F2-II-1, and F2-II-2), one heterozygous carrier (F2-I-1), one unaffected family member (F2-I-2), and four unrelated controls. Platelets from a patient carrying the FLI1 p.R337Q variant represents the MYH10 positive control. GAPDH was used as a protein loading control. Quantification of band intensity for MYH10 is shown below the western blot.

in platelets from the three probands and one carrier of a *FLI1* variant as previously reported.¹⁸ MYH10 protein was also present in the mother of the F2 probands (F2-I-1), albeit at relatively reduced levels (Figure 4E). The polyploidization defect has been shown associated through deregulation of cyclin D1-Cdk4 or CDC6 expression.^{10,12} In MSR cells, GATA1 wild-type or mutants' transfection did not alter their expression levels (Figure S6).

3.9 | Evidence of a *MYH10* intronic regulatory region

Our data suggest that GATA1 regulates *MYH10* expression. Therefore, we obtained GATA1, RUNX1, and FLI1 chromatin immunoprecipitation (ChIP)-sequence data on primary human MKs (deposited by the Göttgens laboratory) from the Gene Expression Omnibus database.¹⁹ The peak enrichments on chromosome 17, which includes the *MYH10* locus, were extracted and displayed in the UCSC genome browser. This analysis showed two enriched binding regions for the GATA1, RUNX1, and FLI1 transcription factors in the *MYH10* gene (displayed from ENCODE data using the erythro-leukemia K562 cell line known to express GATA1) (Figure 5A).

The first binding peak (Chr. 17: 8472947-8473157) located in the *MYH10* 3' untranslated region (UTR) corresponded to GATA1 and RUNX1 binding sites. Remarkably, sequence analysis did not retrieve the consensus GATA1-binding motif in this region. The second peak (Chr. 17: 8553047-8553739) was located within an intronic region and contained potential binding sites for GATA1, FLI1, and RUNX1. Four potential GATA1-binding sites (referred to as BS-1, BS-2, BS-3, and BS-4) were identified, of which three contain the reverted sequence TATC (BS-2, BS-3, and BS-4) (Figure S7). We also uploaded the chromatin interaction analysis with paired-end tag sequencing data for CTCF and POL2 performed on the K562 cell line from ENCODE, using the UCSC genome browser. This analysis revealed that the intronic enhancer was indeed not occupied by Pol2 or CTCF (data not shown). The interaction between gene regulatory regions (displayed with data from ENCODE) revealed that the intronic site was likely within a close chromatin region in a DNA repressive loop between two CTCF enriched regions (data not shown).

3.10 | Transcriptional activity of the *MYH10* intronic element

We compared the 3' UTR and intronic regulatory element-driven expression of *MYH10* using a luciferase reporter assay in two cell lines expressing or not the GATA1 hematopoietic partners. The HEL cell line expresses the GATA1, RUNX1, and FLI1 transcription factors. In HEL cells, both the 3' UTR and intronic regions significantly repressed luciferase expression compared with the pGL3 empty vector (control) (Figure 5B). Removal of only one of the four GATA1-binding sites in *MYH10* intron 8 region was sufficient to yield markedly reduced intronic activity.

We then look at the effect of GATA1 variant on intron 8 driven *MYH10* expression. Because HEL cells express endogenous GATA1 we used a nonhematopoietic model, the MSR epithelial cells, which do not express basal levels of GATA1, RUNX1, and FLI1 (Figure S7). In this model wild-type GATA1 transfection enhanced luciferase activity via the *MYH10* intronic region (Figure 5C left), but not via the 3' UTR region (Figure 5C right). Disruption of all four GATA-binding sites in the intronic region yielded a significant reduction in luciferase activity (approximately 40%). Disruption of BS-2 (M2) or BS-4 (M4) also led to a significant reduction in luciferase activity, while disruption of BS-1 (M1) or BS-3 (M3) did not exhibit any significant effect (Figure 5C left).

We then evaluated the variants effects in MSR cells. Both here reported (N206L and L268M GATA1) and already described (V205M and G208S) GATA1 variants were associated with a marked reduction in transcriptional activity compared with wild-type GATA1 (Figure 5D and Figure S8).

4 | DISCUSSION

In this study, we assessed two pedigrees displaying a variant in the *GATA1* gene. We report the first description of a variant in the C-terminal ZF of GATA1 that initially manifested as mucocutaneous bleeding with platelet dysfunction but without thrombocytopenia, which appeared later in life. We observed increased *MYH10* levels in platelets, thus highlighting the persistence of *MYH10* expression during MK differentiation, which may explain the decrease in MK ploidy and reduced platelet formation. Assessing published ChIP-sequence data and using reporter cell and mutagenesis assays, we demonstrated that GATA1 repressed *MYH10* expression via intronic binding sites in the *MYH10* gene.

To date, nearly all reported GATA1 variants have been shown to involve the N-terminal ZF (positions 205, 208, 216, and 218) and the intron/exon boundaries of exon 2,²⁴ with the exception of the terminal p.X414R variant, which causes removal of the terminal codon and adds 42 extra amino acids to the full-length GATA1 protein.²⁵ Variants in the N-terminal ZF and at position 414 are associated with thrombocytopenia, whereas variants in exon 2 essentially lead to changes in the red blood cell lineage, leading to severe anemia or Diamond-Blackfan anemia. Currently, variants in the C-terminal ZF have not been described. The p.H289R variant, localized immediately 3' of the C-terminal ZF, has been reported to be not as damaging as variants affecting the N-terminal ZF domain.²⁶

In this study, we describe two novel GATA1 variants. The patient harboring the variant at position 206 suffered from moderate bleeding with severe thrombocytopenia and mild dyserythropoietic features. This observation agrees with previous descriptions of N-terminal ZF variants. Accordingly, this variation impairs FOG1 binding. The second variant identified affected the C-terminal ZF. Unlike variations in the N-terminal ZF, the p.L268M variation does not affect the GATA1/FOG1 interaction. The clinical characteristics resemble those observed with the p.R216Q variant localized

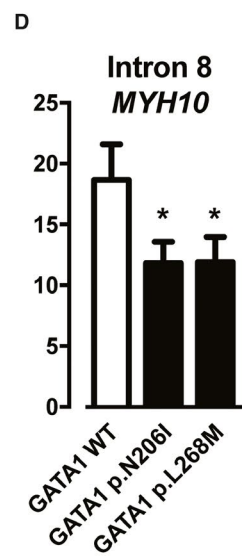
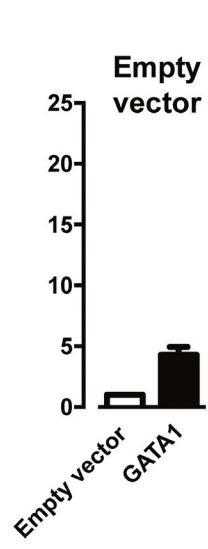
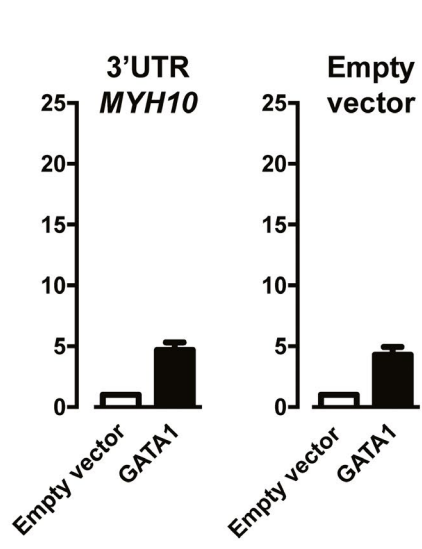
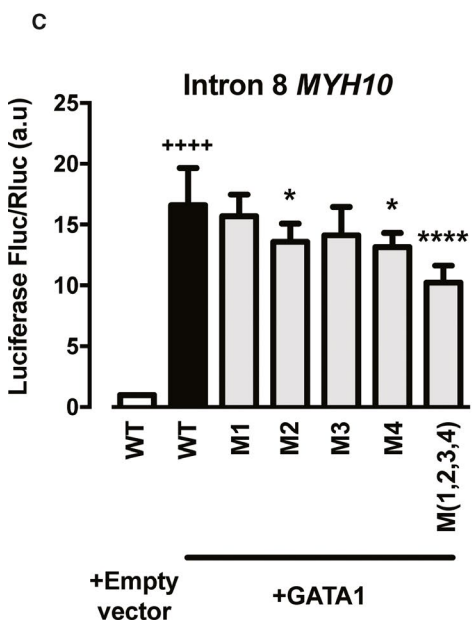
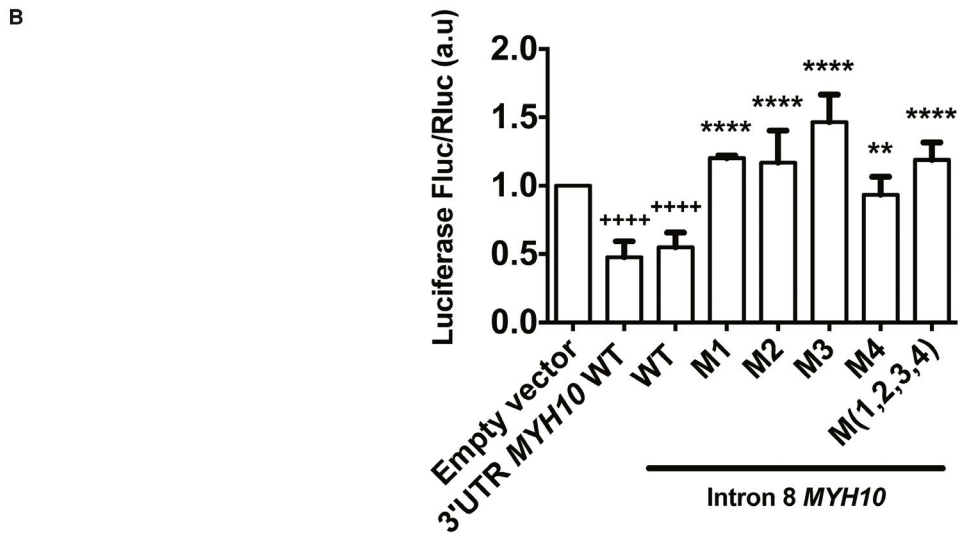
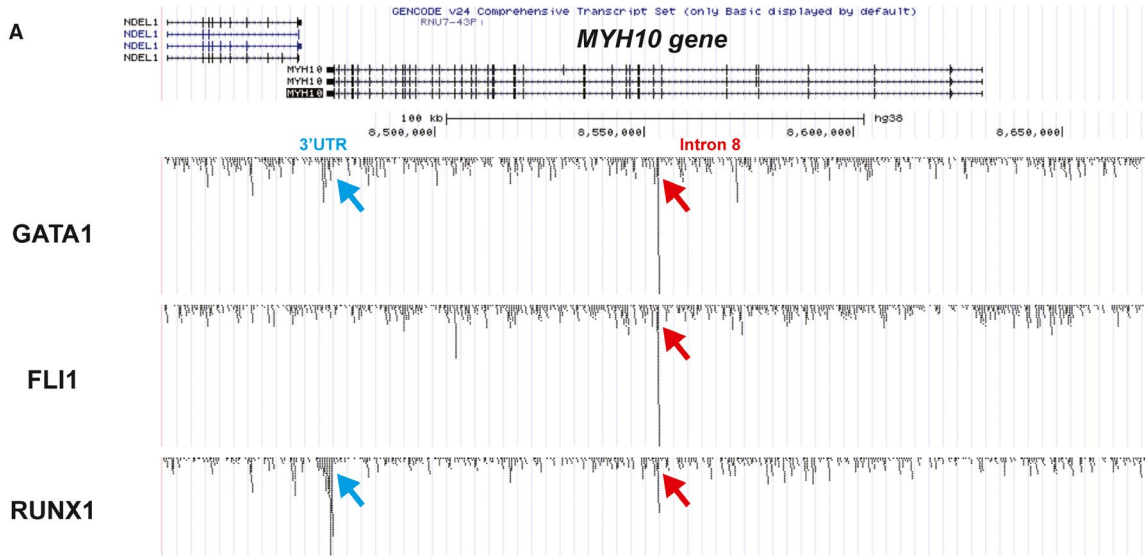


FIGURE 5 Identification and functional analysis of the MYH10 regulatory regions. A, Visualization of MYH10 regulatory regions with GATA1, FLI1, and RUNX1 binding peaks identified via chromatin immunoprecipitation-sequencing. Part of the NDEL gene is shown upstream of the MYH10 gene using the UCSC genome browser (chr17:8,435,074-8,669,900 using GRCh38/hg38). The bottom layer shows the position of two GATA1-binding region peaks within the 3' UTR (untranslated transcribed region, blue arrows) and intron 8 (red arrows) of MYH10 for the transcription factors GATA1, FLI1, and RUNX1. B, Luciferase expression in HEL cells transfected with different pGL3 luciferase reporter vectors including the 3' UTR or intron 8 regions of MYH10 gene. Mutations on GATA1-binding sites in intron 8 were introduced as indicated (M1 or M2 or M3 or M(1,2,3,4)). The pGL3 vector without regulatory regions (empty vector) was used as a control. Each plasmid was assayed in three to seven independent transfection experiments. The dual luciferase assay was performed by sequentially measuring the firefly and Renilla luciferase activities of the same sample with the results expressed as the ratio of firefly to Renilla activity (Fluc/Rluc). $^{**}p < 0.001$, $^{***}p < 0.0001$ vs. pGL3-intron 8 MYH10 wild-type (WT) (one-way ANOVA corrected for multiple comparisons). $^{+++}p < 0.0001$ vs. pGL3-empty vector (one-way ANOVA corrected for multiple comparisons). C, Luciferase expression in GripTite 293 MSR cells transfected with different pGL3 luciferase reporters and pCDNA3-GATA1 vectors as indicated. Left: pGL3-intron 8 MYH10 wild-type (WT), pGL3-intron 8 MYH10 mutants, empty pCDNA3 and pCDNA3-GATA1 WT. Middle: pGL3-3' UTR MYH10, empty pCDNA3, and pCDNA3-GATA1 WT. Right: empty pGL3, empty pCDNA, and pCDNA-GATA1 WT. The pCDNA3 empty vector was used as a control. $^{*}p < 0.01$, $^{****}p < 0.0001$ vs. pGL3-intron8-MYH10 WT in the presence of GATA1 (black bar) (one-way ANOVA corrected for multiple comparisons). $^{++++}p < 0.0001$ vs. the empty pGL3 vector in the absence of GATA1 (white bar). Each plasmid was assayed in six separate transfection experiments (one-way ANOVA corrected for multiple comparisons). D, Luciferase expression after transfection in GripTite 293 MSR cells with pGL3-intron 8 MYH10 WT and pCDNA3-GATA1 WT or variant vectors as indicated. $^{*}p < 0.01$ vs. GATA1 WT (one-way ANOVA corrected for multiple comparisons). Each plasmid was assayed in five separate transfection experiments

in the DNA-binding surface of the N-terminal ZF, including macrothrombocytopenia, red blood cell abnormalities, and minor beta-thalassemia.²⁷⁻³⁰ Presentation was also close to the one described for the H289R variation. As in the F2 patients, the hemizygous males harboring the H289R substitution exhibit increased MCV but normal hemoglobin levels. Thrombocytopenia was present only in two of the four affected family members.²⁶ Although both F2 children presented with high level of fetal hemoglobin, the absence of thrombocytopenia did not initially direct toward a GATA1-related disease. Indeed, the disease initially manifested as severe mucocutaneous bleeding associated with reduced platelet aggregation without thrombocytopenia. Platelet exploration carried out on several occasions did not make it possible to link the platelet phenotype to a known thrombopathy. Indeed, GPIIb/IIIa was expressed at a normal level and was able to bind PAC1 antibody after activation by 10 μ M ADP. No sign of immune deficiency was observed in these children excluding a kindlin 3 deficiency.³¹ Finally, the results of platelet aggregation were not in favor of a CalDAG-GEFI deficiency because platelet activation induced by a high concentration of arachidonic acid, identical to the one used in this article, usually gives normal results.³² For a long time, these children were considered to be carriers of a storage pool disease because of the early detection of a severe deficit of dense granules. These results are to be connected with those of White *et al.*,³³ who observed a near absence of dense bodies in the platelets from a patient with the R216Q GATA1 mutation. Although rescue experiments have not been performed and causality has not been shown, our results support the idea that the spectrum of GATA1-related diseases may be extended to include X-linked bleeding diathesis without thrombocytopenia, associated with collagen and arachidonic acid aggregation defects. In contrast to studies in Gata1-deficient mice,^{9,11,29,34} we did not observe reduced protein levels of GPVI, SYK, or other key molecules involved in collagen signaling pathways, such as PLC γ 2 that could explain the aggregation defect. The decrease in TBXAS1 levels observed in the two F2 brothers may play a role in the reduced response to

arachidonic acid. However, the platelets also failed to respond to U46619, indicating a more complex mechanism. The granule deficiency observed in the current study may also contribute to the platelet aggregation defects, although a complete lack of arachidonic acid- or collagen-induced platelet aggregation is not a feature of granule deficiency. Overall, further studies are required to understand the cause of platelet dysfunction observed in GATA1 variant carriers. Thrombocytopenia developed gradually over time associated with an enlargement in red blood cells, indicating progression of the disease in p.L268M carriers. Cell-type-specific gene regulation may change during ontogeny. There are substantial developmental differences between neonates and adults in the process of megakaryopoiesis and in their responses to TPO.³⁵ Wenqing and colleagues have highlighted fundamental and conserved differences at distinct developmental stages, characterized by simpler promoter-centric regulation of cell-type-specific genes in embryonic cells and increased combinatorial enhancer-driven control in adult cells.³⁶ Overall, the delayed onset of thrombocytopenia observed in the F2 family suggest developmental stage-specific GATA-1 regulation.

Assessment of MKs in GATA1 variant carriers revealed polyploidization and differentiation defects. Assessment of the p.N206I variant revealed a marked decrease in mature CD41^{high}CD42a^{high} MKs, along with an increase in CD41⁻CD42a⁻ cells. Although we cannot formally exclude impaired expression of CD41 and CD42a in MKs harboring a GATA1 variant, the reduction in high-ploidy cells confirmed the MK maturation defect.

Additionally, the GATA1 N206I carrier displayed an increase in circulating CD34⁺ progenitor cells, as described for individuals carrying a germline ETV6 variants.³⁷ Recently, Shin *et al.*³⁸ have found that Gata1 low megakaryocyte-erythroid progenitors/megakaryocyte precursors cell lines display accelerated replication after approximately 90 to 100 days of culture. The observed increase in CD34⁺ cells may reflect this high proliferative capacity.

The polyploidization defect associated with GATA1 is not well understood. MYH10 has been shown to be required for cytokinesis

during meiotic cell division³⁹ and to contribute to MK polyploidisation.^{13,40} RUNX1-mediated silencing of *MYH10* has been found to be required for MK polyploidization and may serve as a biomarker of RUNX1 variants in patients.¹⁵ FLI1 forms a complex with RUNX1 to regulate megakaryopoiesis. Carriers of *FLI1* variants also exhibit elevated MYH10 levels in platelets.¹⁵⁻¹⁷ Interestingly, using a genome-wide analysis of simultaneous transcription factor binding in human MKs and ENCODE ChIP-sequence data, we have shown that FLI1, RUNX1, and GATA1 accumulate at regulatory elements in intron 8 and the 3' UTR of the *MYH10* gene.¹⁹ Additionally, these transcription factors cooperate during megakaryopoiesis as components of a large transcriptional complex,^{21,41} thereby suggesting that GATA1 may regulate MYH10 expression in cooperation with RUNX1 and FLI1. To our knowledge, *MYH10* has not yet been described as a target gene of GATA1. We observed abnormal persistence of MYH10 protein in the platelets of the three *GATA1* variant carriers. The mother of the two F2 brothers also exhibited a slight increase in MYH10 levels. In a reporter luciferase assay using the HEL cell line, both regulatory elements in intron 8 and the 3' UTR of *MYH10* were found to be functional by inducing reduced transcriptional activity. Disruption of the four intronic binding sites fully reversed the repressive activity, indicating that the intronic binding sites are required for *MYH10* repression, despite the presence of the other repressive complex partners (i.e., RUNX1, FLI1). The 3' UTR region of *MYH10* may preferentially bind to a portion of a protein complex that includes GATA1 without binding directly to GATA1. Although GATA1 wild-type enhanced luciferase activity via the MYH10 intronic region in MSR cells, the opposite effect was observed in HEL cells. GATA1 is known to have both activating and repressing activity depending on the cellular and promoter/enhancer context.⁴² Variations in the expression of GATA1 partners in these two cell models, such as RUNX1 and FLI1, may explain these differences. In MSR cells, the GATA1 responsive activity decreased in presence of each variant, compared with wild-type GATA1, indicating that the increase in MYH10 levels observed in patients likely results from reduced interaction between the product of the *GATA1* variants and the *MYH10* intronic region. Intronic GATA1 binding sites have already been shown to be involved in the regulation of 5-aminolevulinic acid synthase 2 (*ALAS2*) gene expression, which is involved in heme synthesis in erythroid cells.⁴³

In summary, we describe two novel pathogenic variations in the *GATA1* gene characterized by distinct clinical and laboratory findings. Our results suggest that variants affecting the *GATA1* C-terminal ZF should likely be assessed in patients with normal platelet counts and platelet aggregation defects in response to collagen and arachidonic. Importantly, both *GATA1* variants analyzed in this study led to persistent expression of MYH10 in platelets. We identify a *MYH10* intronic region that functions as a GATA1-responsive cis-regulatory element.

ACKNOWLEDGMENTS

The study was funded by the "Fondation pour la Recherche Médicale" (granted to P.S.: FDM20150633607), the French Foundation for Rare Diseases (grant WES 2012-2001), The National

Institutes of Diabetes, Digestive and Kidney Diseases (NIDDK) of the National Institutes of Health (granted to J.V.A.: DK101628). The authors acknowledge the members of the French Reference Center for Inherited Hereditary Platelet Disorders (CRPP) for their contribution to clinical analysis of the patients and Dr. M. Fiore for providing patient samples.

CONFLICT OF INTEREST

The authors have declared that no conflict of interest exists.

AUTHOR CONTRIBUTIONS

Paul Saultier, Sandrine Cabantous and Michel Puceat designed and performed the experiments, analyzed the data, and wrote the manuscript. Delphine Potier, Dominique Payet-Bornet, Marjorie Poggi, Franck Peiretti, and Matthias Canault analyzed the data and revised the manuscript. Noémie Saut performed DNA sequencing and revised the manuscript. Jean-Claude Bordet performed TEM analysis and revised the manuscript. Johannes van Agthoven performed the structure analysis experiments and revised the manuscript. Denis Bernot, Marie Loosveld, Céline Falaise, and Pierre Emmanuel Morange performed clinical and biological characterization of patients, analyzed the data, and revised the manuscript. Marjorie Poggi and Marie-Christine Alessi supervised the study and wrote the manuscript.

ORCID

Paul Saultier  <https://orcid.org/0000-0002-6327-0898>

Michel Puceat  <https://orcid.org/0000-0001-9055-7563>

Franck Peiretti  <https://orcid.org/0000-0001-7198-0534>

Matthias Canault  <https://orcid.org/0000-0002-7880-5250>

Dominique Payet-Bornet  <https://orcid.org/0000-0003-3196-3814>

Delphine Potier  <https://orcid.org/0000-0003-1684-9888>

Pierre-Emmanuel Morange  <https://orcid.org/0000-0002-9065-722X>

Marie-Christine Alessi  <https://orcid.org/0000-0003-3927-5792>

Marjorie Poggi  <https://orcid.org/0000-0001-6331-9682>

REFERENCES

1. Crispino JD. GATA1 in normal and malignant hematopoiesis. *Semin Cell Dev Biol.* 2005;16:137-147.
2. Crispino JD, Horwitz MS. GATA factor mutations in hematologic disease. *Blood.* 2017;129:2103-2110.
3. Songdej N, Rao AK. Hematopoietic transcription factor mutations: important players in inherited platelet defects. *Blood.* 2017;129:2873-2881.
4. Ko LJ, Engel JD. DNA-binding specificities of the GATA transcription factor family. *Mol Cell Biol.* 1993;13:4011-4022.
5. Mehaffey MG, Newton AL, Gandhi MJ, Crossley M, Drachman JG. X-linked thrombocytopenia caused by a novel mutation of GATA-1. *Blood.* 2001;98:2681-2688.
6. Nichols KE, Crispino JD, Poncz M, et al. Familial dyserythropoietic anaemia and thrombocytopenia due to an inherited mutation in GATA1. *Nat Genet.* 2000;24:266-270.
7. Chang AN, Cantor AB, Fujiwara Y, et al. GATA-factor dependence of the multitype zinc-finger protein FOG-1 for its essential role in megakaryopoiesis. *Proc Natl Acad Sci USA.* 2002;99:9237-9242.

8. Shivdasani RA, Fujiwara Y, McDevitt MA, Orkin SH. A lineage-selective knockout establishes the critical role of transcription factor GATA-1 in megakaryocyte growth and platelet development. *EMBO J*. 1997;16:3965-3973.
9. Vyas P, Ault K, Jackson CW, Orkin SH, Shivdasani RA. Consequences of GATA-1 deficiency in megakaryocytes and platelets. *Blood*. 1999;93:2867-2875.
10. Muntean AG, Pang L, Poncz M, Dowdy SF, Blobel GA, Crispino JD. Cyclin D-Cdk4 is regulated by GATA-1 and required for megakaryocyte growth and polyploidization. *Blood*. 2007;109:5199-5207.
11. Meinders M, Hoogenboezem M, Scheenstra MR, et al. Repercussion of megakaryocyte-specific gata1 loss on megakaryopoiesis and the hematopoietic precursor compartment. *PLoS One*. 2016;11:e0154342.
12. Mazzi S, Lordier L, Debili N, Raslova H, Vainchenker W. Megakaryocyte and polyploidization. *Exp Hematol*. 2018;57:1-13.
13. Lordier L, Bluteau D, Jalil A, et al. RUNX1-induced silencing of non-muscle myosin heavy chain IIB contributes to megakaryocyte polyploidization. *Nat Commun*. 2012;3:717.
14. Bluteau D, Glembofsky AC, Raimbault A, et al. Dysmegakaryopoiesis of FPD/AML pedigrees with constitutional RUNX1 mutations is linked to myosin II deregulated expression. *Blood*. 2012;120:2708-2718.
15. Antony-Debré I, Bluteau D, Itzykson R, et al. MYH10 protein expression in platelets as a biomarker of RUNX1 and FLI1 alterations. *Blood*. 2012;120:2719-2722.
16. Stockley J, Morgan NV, Bem D, et al. Enrichment of FLI1 and RUNX1 mutations in families with excessive bleeding and platelet dense granule secretion defects. *Blood*. 2013;122:4090-4093.
17. Stevenson WS, Rabbolini DJ, Beutler L, et al. Paris-Trousseau thrombocytopenia is phenocopied by the autosomal recessive inheritance of a DNA-binding domain mutation in FLI1. *Blood*. 2015;126:2027-2030.
18. Saultier P, Vidal L, Canault M, et al. Macrothrombocytopenia and dense granule deficiency associated with FLI1 variants: ultrastructural and pathogenic features. *Haematologica*. 2017;102:1006-1016.
19. Tijssen MR, Cvejic A, Joshi A, et al. Genome-wide analysis of simultaneous GATA1/2, RUNX1, FLI1, and SCL binding in megakaryocytes identifies hematopoietic regulators. *Dev Cell*. 2011;20:597-609.
20. Xu G, Kanazaki R, Toki T, et al. Physical association of the patient-specific GATA1 mutants with RUNX1 in acute megakaryoblastic leukemia accompanying Down syndrome. *Leukemia*. 2006;20:1002-1008.
21. Elagib KE, Racke FK, Mogass M, Khetawat R, Delehanty LL, Goldfarb AN. RUNX1 and GATA-1 coexpression and cooperation in megakaryocytic differentiation. *Blood*. 2003;101:4333-4341.
22. Booth NA, Simpson AJ, Croll A, Bennett B, MacGregor IR. Plasminogen activator inhibitor (PAI-1) in plasma and platelets. *Br J Haematol*. 1988;70:327-333.
23. Bergemalm D, Ramström S, Kardeby C, et al. Platelet proteome and function in X-linked thrombocytopenia with thalassemia and in silico comparisons with gray platelet syndrome. *Haematologica*. 2020; Online ahead of print.
24. Kobayashi E, Shimizu R, Kikuchi Y, Takahashi S, Yamamoto M. Loss of the Gata1 gene IE exon leads to variant transcript expression and the production of a GATA1 protein lacking the N-terminal domain. *J Biol Chem*. 2010;285:773-783.
25. Singleton BK, Roxby DJ, Stirling JW, et al. A novel GATA1 mutation (Stop414Arg) in a family with the rare X-linked blood group Lu(a-b-) phenotype and mild macrothrombocytopenia. *Br J Haematol*. 2013;161:139-142.
26. Pereira J, Bento C, Manco L, Gonzalez A, Vagace J, Ribeiro ML. Congenital dyserythropoietic anemia associated to a GATA1 mutation aggravated by pyruvate kinase deficiency. *Ann Hematol*. 2016;95:1551-1553.
27. Yu C, Nikan KK, Matsushita M, Stamatoyannopoulos G, Orkin SH, Raskind WH. X-linked thrombocytopenia with thalassemia from a mutation in the amino finger of GATA-1 affecting DNA binding rather than FOG-1 interaction. *Blood*. 2002;100:2040-2045.
28. Balduino CL, Pecci A, Loffredo G, et al. Effects of the R216Q mutation of GATA-1 on erythropoiesis and megakaryocytopoiesis. *Thromb Haemost*. 2004;91:129-140.
29. Hughan SC, Senis Y, Best D, et al. Selective impairment of platelet activation to collagen in the absence of GATA1. *Blood*. 2005;105:4369-4376.
30. Åström M, Hahn-Strömberg V, Zetterberg E, Vedin I, Merup M, Palmblad J. X-linked thrombocytopenia with thalassemia displays bone marrow reticulin fibrosis and enhanced angiogenesis: comparisons with primary myelofibrosis. *Am J Hematol*. 2015;90:E44-48.
31. Robert P, Canault M, Farnarier C, et al. A novel leukocyte adhesion deficiency III variant: kindlin-3 deficiency results in integrin- and nonintegrin-related defects in different steps of leukocyte adhesion. *J Immunol*. 2011;186:5273-5283.
32. Canault M, Ghalloussi D, Grosdidier C, et al. Human CalDAG-GEF1 gene (RASGRP2) mutation affects platelet function and causes severe bleeding. *J Exp Med*. 2014;211:1349-1362.
33. White JG, Thomas A. Platelet structural pathology in a patient with the X-linked GATA-1, R216Q mutation. *Platelets*. 2009;20:41-49.
34. Ferreira R, Ohneda K, Yamamoto M, Philipsen S. GATA1 function, a paradigm for transcription factors in hematopoiesis. *Mol Cell Biol*. 2005;25:1215-1227.
35. Liu Z-J, Italiano J Jr, Ferrer-Marin F, et al. Developmental differences in megakaryocytopoiesis are associated with up-regulated TPO signaling through mTOR and elevated GATA-1 levels in neonatal megakaryocytes. *Blood*. 2011;117:4106-4117.
36. Cai W, Huang J, Zhu Q, et al. Enhancer dependence of cell-type-specific gene expression increases with developmental age. *Proc Natl Acad Sci USA*. 2020;117:21450-21458.
37. Poggi M, Canault M, Favier M, et al. Germline variants in ETV6 underlie reduced platelet formation, platelet dysfunction and increased levels of circulating CD34+ progenitors. *Haematologica*. 2017;102:282-294.
38. Shin E, Jeong J-G, Chung H, et al. The Gata1^{low} murine megakaryocyte-erythroid progenitor cells expand robustly and alter differentiation potential. *Biochem Biophys Res Commun*. 2020;528:46-53.
39. Yang F, Wei Q, Adelstein RS, Wang PJ. Non-muscle myosin IIB is essential for cytokinesis during male meiotic cell divisions. *Dev Biol*. 2012;369:356-361.
40. Badirou I, Pan J, Legrand C, et al. Carboxyl-terminal-dependent recruitment of nonmuscle myosin II to megakaryocyte contractile ring during polyploidization. *Blood*. 2014;124:2564-2568.
41. Eisbacher M, Holmes ML, Newton A, et al. Protein-protein interaction between Fli-1 and GATA-1 mediates synergistic expression of megakaryocyte-specific genes through cooperative DNA binding. *Mol Cell Biol*. 2003;23:3427-3441.
42. Welch JJ, Watts JA, Vakoc CR, et al. Global regulation of erythroid gene expression by transcription factor GATA-1. *Blood*. 2004;104:3136-3147.
43. Zhang Y, Zhang J, An W, et al. Intron 1 GATA site enhances ALAS2 expression indispensably during erythroid differentiation. *Nucleic Acids Res*. 2017;45:657-671.

SUPPORTING INFORMATION

Additional supporting information may be found online in the Supporting Information section.

How to cite this article: Saultier P, Cabantous S, Puceat M, et al. GATA1 pathogenic variants disrupt MYH10 silencing during megakaryopoiesis. *J Thromb Haemost*. 2021;19:2287-2301. <https://doi.org/10.1111/jth.15412>